



SINGLE-PARTICLE BATTERY ELECTRODE REPRESENTATION-BASED CAPACITY FADING OF LITHIUM-ION CELLS

Vipin Kakkar^a, Vijander Kumar^b, V.Vibhanshu^c

^a Department of Mechanical Engineering, Indian Institute of Technology, Delhi, India

^b Department of Accessory Design, National Institute of Fashion Technology, Jodhpur, India

^c Mechanical engineering department IITDelhi

ABSTRACT

The single particle modelling is studied for the degradation and its effect on the cyclic performance of lithium-ion cell. Lithium-ion cell degradation is studied as a function of cycle number and parasitic reaction current density. It is shown that in lithium-ion batteries, capacity fade occurring as a result of the formation of solid electrolyte interphase on the negative carbon electrode occurs over a number of cycles due to the slow nature of this electrochemical process. Mathematical modeling is also carried out by single particle model and various degradation mechanisms to validate and study the various aspects of cell capacity deterioration.

Key words: Lithium ion battery; single particle model; capacity fade; solid electrolyte interphase (SEI)

DOI: 10.48047/ecb/2023.12.si12.129

INTRODUCTION:

To simulate the Li-ion batteries capacity fade, a discharge-charge model was developed. Capacity fading of lithium-ion batteries takes place due to side reactions and these side reactions take place due to over-charging and over-discharging of the cell. At the time of charging, when lithium ions travel from positive electrode toward the negative one, they tend to react with carbonate based electrolyte irreversibly to form a layer over the anode surface. Due to this layer, the anode film resistance increases which restricts the intercalation of lithium ions. With time, the formation of the carbonate film leads to loss of useful lithium and hence decreases cell capacity.

Overcharging of battery is responsible for capacity loss to a great extent, as due to overcharging on the positive electrode electrolyte oxidation takes place, whereas on negative electrode lithium deposition take place [1]

Schematic of Lithium-ion cell of single particle is depicted in Figure 1. Positive and negative electrodes are arranged in the system and separator presence is neglected in the single particle model development. Lithium manganese oxide is used as positive electrode and carbon is used as negative electrode. At the time of charging from the positive electrode lithium ions get deintercalated and negative electrode gets intercalated by lithium ions. At the time of discharging reverse process takes place.

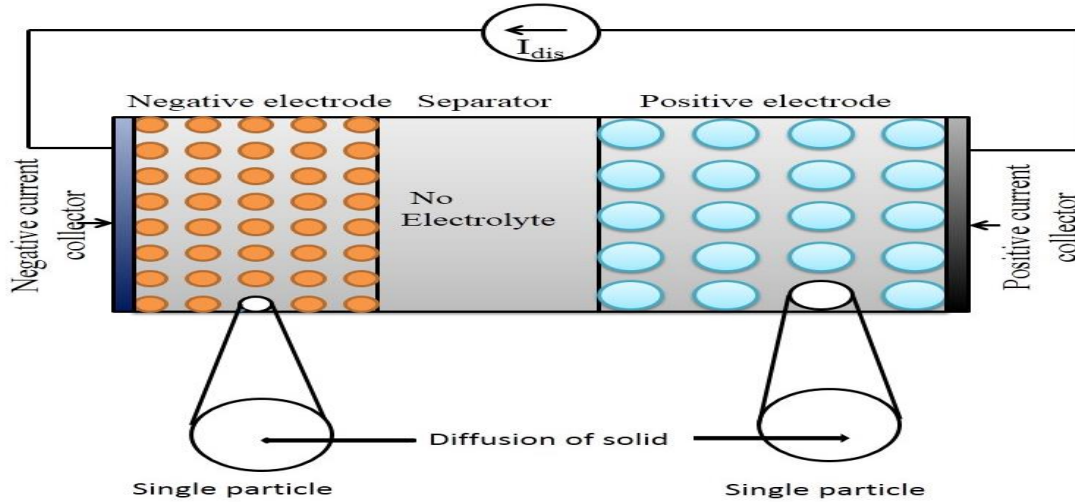


Figure 1: Schematic of Lithium-ion cell of single particle model

Mathematical modelling of single particle with degradation:

A simplified model with capacity fading of lithium ion batteries in single particle model is as follows. The present study aim is to model the film formation parasitic reaction on the anode surface due to cycling only [2]

When the parasitic reaction occurs at the anode/electrolyte interface, across the interface wall flux j , is defined by

$$j_n = j_{int} + j_{para}$$

Here, it is assumed that the local parasitic reaction current density, j_{para} follows a simple Tafel relation [4]

$$j_{para} = -j_{para}^o \exp\left(-\frac{\alpha_c F}{RT} \eta_{para}\right)$$

and

$$\eta_{para} = \phi_s - U_{para} - j_n R_f$$

The wall flux across the interface of anode/electrolyte is equal to the local intercalation/deintercalation current density in the absence of a parasitic reaction.

$$j_n = j_{int}$$

Here, Butler-Volmer equation provides the j_{int} .

$$j_{int} = Fk_n (C_e)^{\frac{1}{2}} (C_{maxn} - C_{sn})^{\frac{1}{2}} (C_{sn})^{\frac{1}{2}} \left(\exp\left(\frac{\alpha_a F}{RT} \eta_{int}\right) - \exp\left(-\frac{\alpha_c F}{RT} \eta_{int}\right) \right)$$

$$\eta_{int} = \phi_s - U_{int} - j_n R_f$$

For the cathode, $R_f = 0$. C_{sn} represents the solid phase lithium concentration at the solid/electrolyte interface, C_{maxn} is the maximum allowable concentration in the solid phase for the negative electrode and R_f is the anode film resistance.[3]

$$R_f = \frac{\delta_f}{\kappa_f}$$

$$\frac{\partial \delta_f}{\partial t} = -\frac{j_{para} M}{\rho F}$$

where M is the molecular weight (kg/mol), ρ is the film density, F is the Faraday's constant, δ_f is the film thickness, and κ denotes the newly formed surface film's electrical conductivity (S/m).

Development of Non-linear Solver

The above model is solved by applying the Newton-Rap son method for multiple variables. The following functions are defined that are used to construct the Jacobian matrix

$$F_1 = j_{para} + j_{para}^o \exp\left(-\frac{F}{2RT} \eta_{para}\right)$$

$$F_2 = \delta_f - \delta_f^0 + \frac{j_{para} M \Delta t}{\rho F}$$

$$F_3 = R_f - \frac{\delta_f}{\kappa}$$

$$F_4 = \eta_{para} - \phi_s + U_{para} + j(R_f + R_f^0)$$

$$F_5 = \eta_{int} - \phi_s + U_{int} + j(R_f + R_f^0)$$

$$F_6 = j_{int} - Fk(C_e)^5(C_{maxn} - C_{sn})^5(C_{sn})^5 \left(\exp\left(\frac{F}{2RT} \eta_{int}\right) - \exp\left(-\frac{F}{2RT} \eta_{int}\right) \right)$$

$$F_7 = j - j_{int} - j_{para}$$

The above function F_1 to F_7 have seven unknown variable j_{para} , δ_f , R_f , η_{para} , ϕ_s , η_{int} , and j_{int} . Each function from F_1 to F_7 is differentiated with respect to each variable to form a Jacobian matrix at each time step. Subsequently, the equations are assembled and a set of linear equations, given by equation are solved.

$$\mathbf{A}_{7 \times 7} (\Delta \mathbf{x})_{7 \times 1} = \mathbf{b}_{7 \times 1}$$

Where $\mathbf{x} = [j_{para} \ \delta_f \ R_f \ \eta_{para} \ \phi_s \ \eta_{int} \ j_{int}]^T$. And matrix $\mathbf{A}_{7 \times 7}$ and $\mathbf{b}_{7 \times 1}$ is shown in Appendix .

The iterative solution process is as follows. First, the initial value of all the seven parameters is defined and the function F_1, F_2, \dots, F_7 is calculated at initial value. Then, by solving equation

(3.41) and adding to the old guessed values, the new value of all the seven parameters is obtained. If the parameters have not converged, the iteration process is repeated until a converged solution is reached for the charging equation of the degradation model.

Results and Discussion

Implementation of SEI formation during charging period with fixed t_d and t_c

The cell potential variation with time considering degradation in the cell with fixed time of discharge and time of charge with each cycle of 7800 sec is shown in Figure 4.8. A MATLAB script is written and run for 100 cycle and 1st, 50th, 100th cycle is compared. The value of $j_0^{\text{para}} = .80 \times 10^{-7} \text{ A/}$

Figure show as the number of cycle increases the cell potential decreases in the discharging portion as shown in the exploded view in part and the value of cell potential increases in the charging in the portion as the number of cycle increase as shown in exploded view in part . The value of cell potential increases due to increase in the in the film resistance. As the value of parasitic reaction current density is very low the side reaction take place very slow due to which the degradation in the cell is very slow. [6]

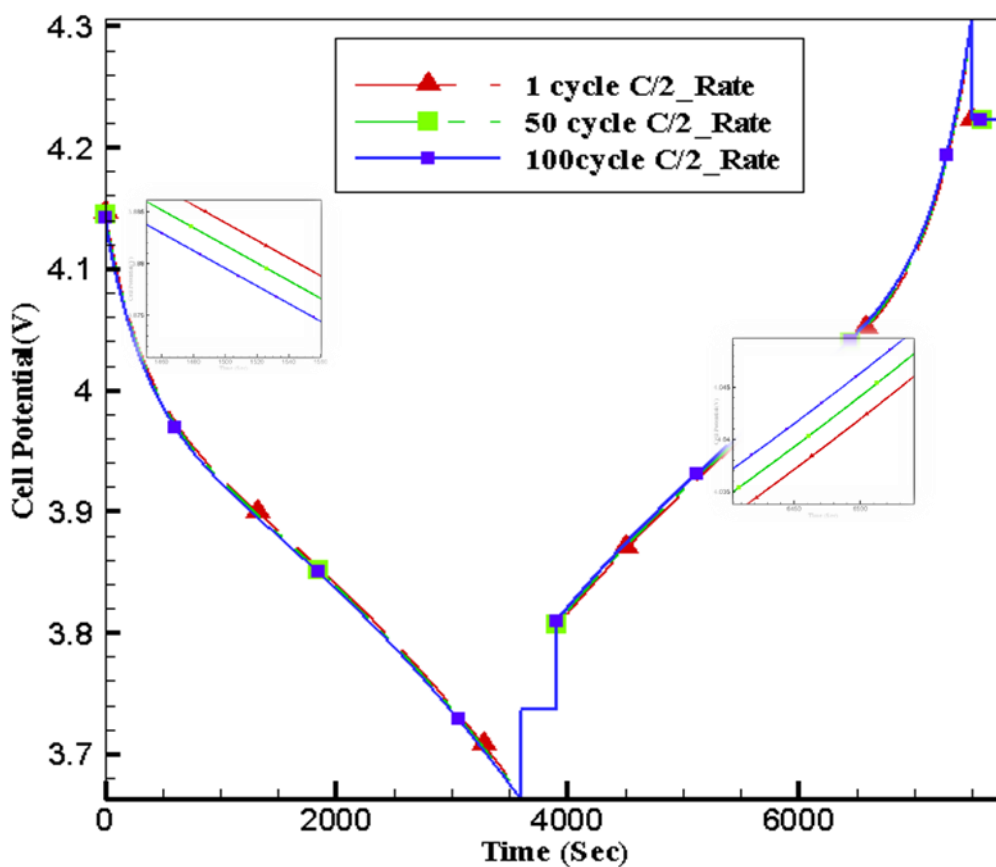


Figure 2:
considerin

Cell pote
parasitic

Figure bel
of active n

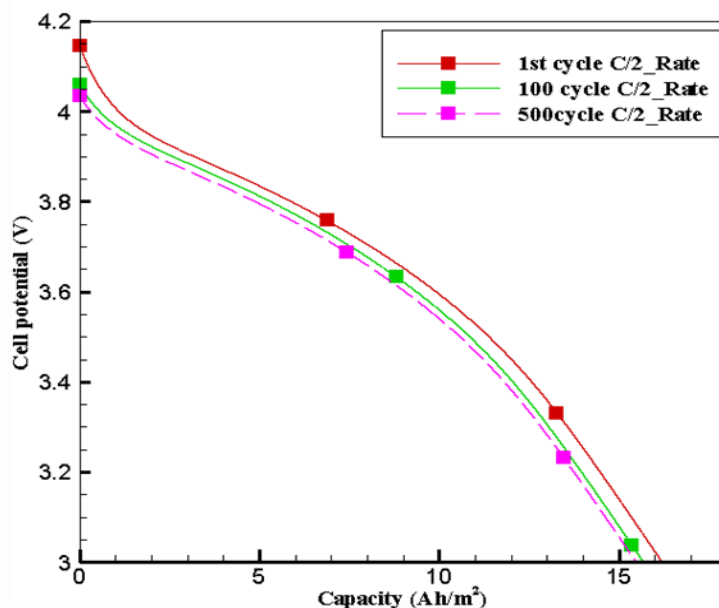


Figure 3: Cell potential variation with capacity at different no cycle considering degradation
Cell potential variation with capacity for different no of cycle with higher value of initial parasitic reaction current density at C/2 rate

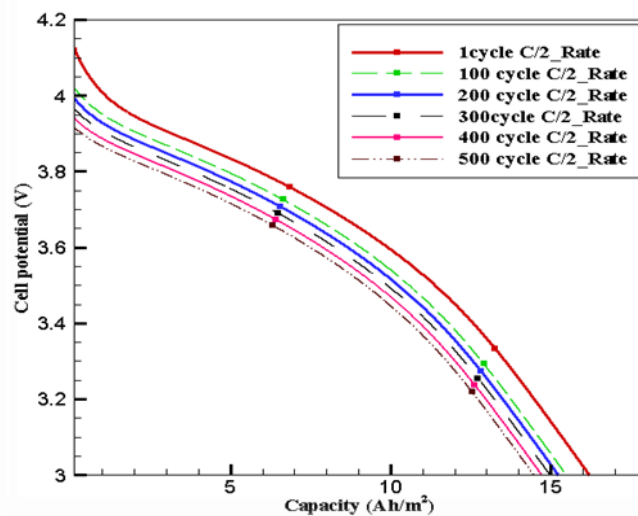


Figure 4: Cell potential variation with capacity at different no cycle considering degradation.
Above figure show cell potential variation with capacity at different cycle for C/2 rate the cell potential and capacity rate decreases as number of cycle increases, as the number of cycle increases, there is an increase in the film resistance at the electrode surface.

Conclusion

In this work, a model of Charge- discharge capacity fade was developed by considering degradation in the model. The model is solved by using numerical method technique Newton

Rapson method for multiple variable using MATLAB code. The degradation model is run for different no cycle and varying the value of initial parasitic reaction current density to study the capacity loss. As the number of cycling increases the capacity decreases because of side reaction over the surface of negative electrode. The anode surface film resistance increases because in parasitic reaction insoluble products gets precipitated which restricts the movement of Li ion. Due to the side reaction product formed with cycling, it cause the dropping of discharge voltage with cycling. With increasing film resistance of the anode surface and charge /discharge rate resulted in incomplete charging of the cell.

NOMENCLATURE

| | |
|--------------|--|
| j_{int} | intercalation current density (A/m²) |
| j_{para} | current density of parasitic reaction (A/m²) |
| j_{para}^0 | initial state parasitic reaction current density (A/m²) |
| k_j | lithium intercalation/deintercalation rate constant (Am^{2.5}/(Cmol^{2.5})) |
| M | molecular weight (kg/mol) |
| L_j | electrode length ‘j’ |
| r | radial coordinate (m) |
| R | universal gas constant (8.314 J/(mol K)) |
| R_j | particle radius (m) |
| R_f | film resistance at anode (Ωm^2) |
| T | temperature (K) |
| t | time(Sec) |
| t_c | time of charge (sec) |
| t_d | discharging time (sec) |

References

- [1]. D.Zhang, B.Haran, a Durairajan,R.White,Y.Podrazhansky,and B.N.Popov,“Studies on capacity fade of lithium-ion batteries ”, *Journal of Power Sources*, vol. 91, no.2, pp. 122-129, (2000).
- [2] . P.Arora, R.E.White ,S. Carolina, and M.Doyle, “ Capacity Fade Mechanisms and side reaction in lithium ion batteries” , *Journal of The Electrochemical Society* ,vol.145, no.10, pp 3647-3667, (1998).
- [3]. Gang Ning,Ralph E.White, Branko N.Popov, “A generalized cycle life model of rechargeable Li-ion batteries”*Electrochimica Acta*,2012-2022, (2006).
- [4].K. B. Oldham and J. C. Myland, “Fundamentals of Electrochemical Science”, 1st ed., Academic Press, California (1993).
- [5]. S.Santhanagopalan, Q.Guo, P.Ramadass, “Review of models for predicting the cyclic performance of lithium ion batteries”, *Journal of Power Sources*, vol. 156, no.2, pp. 620-680, (2006)

- [6]. Gang Ning, Branko N. Popov, "Cycle Life Modelling of Lithium Ion Batteries", *Journal of The Electrochemical Society*, vol. 151, no. 10, pp. 1584-1591, (2004)
- [7]. D. Zhang, B. Haran, a Durairajan, R. White, Y. Podrazhansky, and B. N. Popov, "Studies on capacity fade of lithium-ion batteries", *Journal of Power Sources*, vol. 91, no. 2, pp. 122-129, (2000).
- [8]. S. K. Rahimian, S. Rayman, R. White, "Extension of physics based single particle model for higher charge-discharge rates", *Journal of Power Sources*, vol. 224, pp. 180-194 (2013).

APPENDIX A

A2: Matrix $A_{7 \times 7}$ is given below

$$\begin{bmatrix} \frac{\partial F_1}{\partial j_{int}} & \frac{\partial F_1}{\partial j_{para}} & \frac{\partial F_1}{\partial \eta_{para}} & \frac{\partial F_1}{\partial \eta_{int}} & \frac{\partial F_1}{\partial \phi_s} & \frac{\partial F_1}{\partial R_f} & \frac{\partial F_1}{\partial \delta_f} \\ \frac{\partial F_2}{\partial j_{int}} & \frac{\partial F_2}{\partial j_{para}} & \frac{\partial F_2}{\partial \eta_{para}} & \frac{\partial F_2}{\partial \eta_{int}} & \frac{\partial F_2}{\partial \phi_s} & \frac{\partial F_2}{\partial R_f} & \frac{\partial F_2}{\partial \delta_f} \\ \frac{\partial F_3}{\partial j_{int}} & \frac{\partial F_3}{\partial j_{para}} & \frac{\partial F_3}{\partial \eta_{para}} & \frac{\partial F_3}{\partial \eta_{int}} & \frac{\partial F_3}{\partial \phi_s} & \frac{\partial F_3}{\partial R_f} & \frac{\partial F_3}{\partial \delta_f} \\ \frac{\partial F_4}{\partial j_{int}} & \frac{\partial F_4}{\partial j_{para}} & \frac{\partial F_4}{\partial \eta_{para}} & \frac{\partial F_4}{\partial \eta_{int}} & \frac{\partial F_4}{\partial \phi_s} & \frac{\partial F_4}{\partial R_f} & \frac{\partial F_4}{\partial \delta_f} \\ \frac{\partial F_5}{\partial j_{int}} & \frac{\partial F_5}{\partial j_{para}} & \frac{\partial F_5}{\partial \eta_{para}} & \frac{\partial F_5}{\partial \eta_{int}} & \frac{\partial F_5}{\partial \phi_s} & \frac{\partial F_5}{\partial R_f} & \frac{\partial F_5}{\partial \delta_f} \\ \frac{\partial F_6}{\partial j_{int}} & \frac{\partial F_6}{\partial j_{para}} & \frac{\partial F_6}{\partial \eta_{para}} & \frac{\partial F_6}{\partial \eta_{int}} & \frac{\partial F_6}{\partial \phi_s} & \frac{\partial F_6}{\partial R_f} & \frac{\partial F_6}{\partial \delta_f} \\ \frac{\partial F_7}{\partial j_{int}} & \frac{\partial F_7}{\partial j_{para}} & \frac{\partial F_7}{\partial \eta_{para}} & \frac{\partial F_7}{\partial \eta_{int}} & \frac{\partial F_7}{\partial \phi_s} & \frac{\partial F_7}{\partial R_f} & \frac{\partial F_7}{\partial \delta_f} \end{bmatrix}$$

A3: Matrix $b_{7 \times 1} = [F_1 \ F_2 \ F_3 \ F_4 \ F_5 \ F_6 \ F_7]^T$ the value of $F_1 \ F_2 \dots \ F_7$ is calculated at guessed value.